CDF/PUB/TOP/CDFR/9664

First Measurement of the $t\bar{t}$ Differential Cross Section $d\sigma/dM_{t\bar{t}}$ in $p\bar{p}$ Collisions at $\sqrt{s} = 1.96$ TeV

T. Aaltonen,[24] J. Adelman,[14] T. Akimoto,[56] B. Álvarez González[s],[12] S. Amerio[y],[44] D. Amidei,[35] A. Anastassov,[39] A. Annovi,[20] J. Antos,[15] G. Apollinari,[18] A. Apresyan,[49] T. Arisawa,[58] A. Artikov,[16] W. Ashmanskas,[18] A. Attal,[4] A. Aurisano,[54] F. Azfar,[43] P. Azzurri[z],[47] W. Badgett,[18] A. Barbaro-Galtieri,[29] V.E. Barnes,[49] B.A. Barnett,[26] V. Bartsch,[31] G. Bauer,[33] P.-H. Beauchemin,[34] F. Bedeschi,[47] D. Beecher,[31] S. Behari,[26] G. Bellettini[z],[47] J. Bellinger,[60] D. Benjamin,[17] A. Beretvas,[18] J. Beringer,[29] A. Bhatti,[51] M. Binkley,[18] D. Bisello[y],[44] I. Bizjak[ee],[31] R.E. Blair,[2] C. Blocker,[7] B. Blumenfeld,[26] A. Bocci,[17] A. Bodek,[50] V. Boisvert,[50] G. Bolla,[49] D. Bortoletto,[49] J. Boudreau,[48] A. Boveia,[11] B. Brau[a],[11] A. Bridgeman,[25] L. Brigliadori,[44] C. Bromberg,[36] E. Brubaker,[14] J. Budagov,[16] H.S. Budd,[50] S. Budd,[25] S. Burke,[18] K. Burkett,[18] G. Busetto[y],[44] P. Bussey,[22] A. Buzatu,[34] K. L. Byrum,[2] S. Cabrera[u],[17] C. Calancha,[32] M. Campanelli,[36] M. Campbell,[35] F. Canelli[14],[18] A. Canepa,[46] B. Carls,[25] D. Carlsmith,[60] R. Carosi,[47] S. Carrillo[n],[19] S. Carron,[34] B. Casal,[12] M. Casarsa,[18] A. Castro[x],[6] P. Catastini[aa],[47] D. Cauz[dd],[55] V. Cavaliere[aa],[47] M. Cavalli-Sforza,[4] A. Cerri,[29] L. Cerrito[o],[31] S.H. Chang,[28] Y.C. Chen,[1] M. Chertok,[8] G. Chiarelli,[47] G. Chlachidze,[18] F. Chlebana,[18] K. Cho,[28] D. Chokheli,[16] J.P. Chou,[23] G. Choudalakis,[33] S.H. Chuang,[53] K. Chung,[13] W.H. Chung,[60] Y.S. Chung,[50] T. Chwalek,[27] C.I. Ciobanu,[45] M.A. Ciocci[aa],[47] A. Clark,[21] D. Clark,[7] G. Compostella,[44] M.E. Convery,[18] J. Conway,[8] M. Cordelli,[20] G. Cortiana[y],[44] C.A. Cox,[8] D.J. Cox,[8] F. Crescioli[z],[47] C. Cuenca Almenar[u],[8] J. Cuevas[s],[12] R. Culbertson,[18] J.C. Cully,[35] D. Dagenhart,[18] M. Datta,[18] T. Davies,[22] P. de Barbaro,[50] S. De Cecco,[52] A. Deisher,[29] G. De Lorenzo,[4] M. Dell'Orso[z],[47] C. Deluca,[4] L. Demortier,[51] J. Deng,[17] M. Deninno,[6] P.F. Derwent,[18] G.P. di Giovanni,[45] C. Dionisi[cc],[52] B. Di Ruzza[dd],[55] J.R. Dittmann,[5] M. D'Onofrio,[4] S. Donati[z],[47] P. Dong,[9] J. Donini,[44] T. Dorigo,[44]

S. Dube,[53] J. Efron,[40] A. Elagin,[54] R. Erbacher,[8] D. Errede,[25] S. Errede,[25] R. Eusebi,[18] H.C. Fang,[29] S. Farrington,[43] W.T. Fedorko,[14] R.G. Feild,[61] M. Feindt,[27] J.P. Fernandez,[32] C. Ferrazza[bb],[47] R. Field,[19] G. Flanagan,[49] R. Forrest,[8] M.J. Frank,[5] M. Franklin,[23] J.C. Freeman,[18] I. Furic,[19] M. Gallinaro,[52] J. Galyardt,[13] F. Garberson,[11] J.E. Garcia,[21] A.F. Garfinkel,[49] K. Genser,[18] H. Gerberich,[25] D. Gerdes,[35] A. Gessler,[27] S. Giagu[cc],[52] V. Giakoumopoulou,[3] P. Giannetti,[47] K. Gibson,[48] J.L. Gimmell,[50] C.M. Ginsburg,[18] N. Giokaris,[3] M. Giordani[dd],[55] P. Giromini,[20] M. Giunta[z],[47] G. Giurgiu,[26] V. Glagolev,[16] D. Glenzinski,[18] M. Gold,[38] N. Goldschmidt,[19] A. Golossanov,[18] G. Gomez,[12] G. Gomez-Ceballos,[33] M. Goncharov,[33] O. González,[32] I. Gorelov,[38] A.T. Goshaw,[17] K. Goulianos,[51] A. Gresele[y],[44] S. Grinstein,[23] C. Grosso-Pilcher,[14] R.C. Group,[18] U. Grundler,[25] J. Guimaraes da Costa,[23] Z. Gunay-Unalan,[36] C. Haber,[29] K. Hahn,[33] S.R. Hahn,[18] E. Halkiadakis,[53] B.-Y. Han,[50] J.Y. Han,[50] F. Happacher,[20] K. Hara,[56] D. Hare,[53] M. Hare,[57] S. Harper,[43] R.F. Harr,[59] R.M. Harris,[18] M. Hartz,[48] K. Hatakeyama,[51] C. Hays,[43] M. Heck,[27] A. Heijboer,[46] J. Heinrich,[46] C. Henderson,[33] M. Herndon,[60] J. Heuser,[27] S. Hewamanage,[5] D. Hidas,[17] C.S. Hill[c],[11] D. Hirschbuehl,[27] A. Hocker,[18] S. Hou,[1] M. Houlden,[30] S.-C. Hsu,[29] B.T. Huffman,[43] R.E. Hughes,[40] U. Husemann,[61] M. Hussein,[36] J. Huston,[36] J. Incandela,[11] G. Introzzi,[47] M. Iori[cc],[52] A. Ivanov,[8] E. James,[18] D. Jang,[13] B. Jayatilaka,[17] E.J. Jeon,[28] M.K. Jha,[6] S. Jindariani,[18] W. Johnson,[8] M. Jones,[49] K.K. Joo,[28] S.Y. Jun,[13] J.E. Jung,[28] T.R. Junk,[18] T. Kamon,[54] D. Kar,[19] P.E. Karchin,[59] Y. Kato[l],[42] R. Kephart,[18] J. Keung,[46] V. Khotilovich,[54] B. Kilminster,[18] D.H. Kim,[28] H.S. Kim,[28] H.W. Kim,[28] J.E. Kim,[28] M.J. Kim,[20] S.B. Kim,[28] S.H. Kim,[56] Y.K. Kim,[14] N. Kimura,[56] L. Kirsch,[7] S. Klimenko,[19] B. Knuteson,[33] B.R. Ko,[17] K. Kondo,[58] D.J. Kong,[28] J. Konigsberg,[19] A. Korytov,[19] A.V. Kotwal,[17] M. Kreps,[27] J. Kroll,[46] D. Krop,[14] N. Krumnack,[5] M. Kruse,[17] V. Krutelyov,[11] T. Kubo,[56] T. Kuhr,[27] N.P. Kulkarni,[59] M. Kurata,[56] S. Kwang,[14] A.T. Laasanen,[49] S. Lami,[47] S. Lammel,[18] M. Lancaster,[31] R.L. Lander,[8] K. Lannon[r],[40] A. Lath,[53] G. Latino[aa],[47] I. Lazzizzera[y],[44] T. LeCompte,[2] E. Lee,[54] H.S. Lee,[14] S.W. Lee[t],[54] S. Leone,[47] J.D. Lewis,[18] C.-S. Lin,[29] J. Linacre,[43] M. Lindgren,[18] E. Lipeles,[46] T.M. Liss,[25] A. Lister,[8] D.O. Litvintsev,[18] C. Liu,[48] T. Liu,[18] N.S. Lockyer,[46] A. Loginov,[61] M. Loreti[y],[44] L. Lovas,[15] D. Lucchesi[y],[44] C. Luci[cc],[52] J. Lueck,[27] P. Lujan,[29]

P. Lukens,[18] G. Lungu,[51] L. Lyons,[43] J. Lys,[29] R. Lysak,[15] D. MacQueen,[34] R. Madrak,[18] K. Maeshima,[18] K. Makhoul,[33] T. Maki,[24] P. Maksimovic,[26] S. Malde,[43] S. Malik,[31] G. Manca[e],[30] A. Manousakis-Katsikakis,[3] F. Margaroli,[49] C. Marino,[27] C.P. Marino,[25] A. Martin,[61] V. Martin[k],[22] M. Martínez,[4] R. Martínez-Ballarín,[32] T. Maruyama,[56] P. Mastrandrea,[52] T. Masubuchi,[56] M. Mathis,[26] M.E. Mattson,[59] P. Mazzanti,[6] K.S. McFarland,[50] P. McIntyre,[54] R. McNulty[j],[30] A. Mehta,[30] P. Mehtala,[24] A. Menzione,[47] P. Merkel,[49] C. Mesropian,[51] T. Miao,[18] N. Miladinovic,[7] R. Miller,[36] C. Mills,[23] M. Milnik,[27] A. Mitra,[1] G. Mitselmakher,[19] H. Miyake,[56] N. Moggi,[6] C.S. Moon,[28] R. Moore,[18] M.J. Morello[z],[47] J. Morlock,[27] P. Movilla Fernandez,[18] J. Mülmenstädt,[29] A. Mukherjee,[18] Th. Muller,[27] R. Mumford,[26] P. Murat,[18] M. Mussini[x],[6] J. Nachtman,[18] Y. Nagai,[56] A. Nagano,[56] J. Naganoma,[56] K. Nakamura,[56] I. Nakano,[41] A. Napier,[57] V. Necula,[17] J. Nett,[60] C. Neu[v],[46] M.S. Neubauer,[25] S. Neubauer,[27] J. Nielsen[g],[29] L. Nodulman,[2] M. Norman,[10] O. Norniella,[25] E. Nurse,[31] L. Oakes,[43] S.H. Oh,[17] Y.D. Oh,[28] I. Oksuzian,[19] T. Okusawa,[42] R. Orava,[24] K. Osterberg,[24] S. Pagan Griso[y],[44] E. Palencia,[18] V. Papadimitriou,[18] A. Papaikonomou,[27] A.A. Paramonov,[14] B. Parks,[40] S. Pashapour,[34] J. Patrick,[18] G. Pauletta[dd],[55] M. Paulini,[13] C. Paus,[33] T. Peiffer,[27] D.E. Pellett,[8] A. Penzo,[55] T.J. Phillips,[17] G. Piacentino,[47] E. Pianori,[46] L. Pinera,[19] K. Pitts,[25] C. Plager,[9] L. Pondrom,[60] O. Poukhov*,[16] N. Pounder,[43] F. Prakoshyn,[16] A. Pronko,[18] J. Proudfoot,[2] F. Ptohos[i],[18] E. Pueschel,[13] G. Punzi[z],[47] J. Pursley,[60] J. Rademacker[c],[43] A. Rahaman,[48] V. Ramakrishnan,[60] N. Ranjan,[49] I. Redondo,[32] P. Renton,[43] M. Renz,[27] M. Rescigno,[52] S. Richter,[27] F. Rimondi[x],[6] L. Ristori,[47] A. Robson,[22] T. Rodrigo,[12] T. Rodriguez,[46] E. Rogers,[25] S. Rolli,[57] R. Roser,[18] M. Rossi,[55] R. Rossin,[11] P. Roy,[34] A. Ruiz,[12] J. Russ,[13] V. Rusu,[18] B. Rutherford,[18] H. Saarikko,[24] A. Safonov,[54] W.K. Sakumoto,[50] O. Saltó,[4] L. Santi[dd],[55] S. Sarkar[cc],[52] L. Sartori,[47] K. Sato,[18] A. Savoy-Navarro,[45] P. Schlabach,[18] A. Schmidt,[27] E.E. Schmidt,[18] M.A. Schmidt,[14] M.P. Schmidt*,[61] M. Schmitt,[39] T. Schwarz,[8] L. Scodellaro,[12] A. Scribano[aa],[47] F. Scuri,[47] A. Sedov,[49] S. Seidel,[38] Y. Seiya,[42] A. Semenov,[16] L. Sexton-Kennedy,[18] F. Sforza,[47] A. Sfyrla,[25] S.Z. Shalhout,[59] T. Shears,[30] P.F. Shepard,[48] M. Shimojima[q],[56] S. Shiraishi,[14] M. Shochet,[14] Y. Shon,[60] I. Shreyber,[37] A. Sidoti,[47] P. Sinervo,[34] A. Sisakyan,[16]

* Deceased

A.J. Slaughter,[18] J. Slaunwhite,[40] K. Sliwa,[57] J.R. Smith,[8] F.D. Snider,[18] R. Snihur,[34] A. Soha,[8] S. Somalwar,[53] V. Sorin,[36] J. Spalding,[18] T. Spreitzer,[34] P. Squillacioti[aa],[47] M. Stanitzki,[61] R. St. Denis,[22] B. Stelzer,[34] O. Stelzer-Chilton,[34] D. Stentz,[39] J. Strologas,[38] G.L. Strycker,[35] D. Stuart,[11] J.S. Suh,[28] A. Sukhanov,[19] I. Suslov,[16] T. Suzuki,[56] A. Taffard[f],[25] R. Takashima,[41] Y. Takeuchi,[56] R. Tanaka,[41] M. Tecchio,[35] P.K. Teng,[1] K. Terashi,[51] J. Thom[h],[18] A.S. Thompson,[22] G.A. Thompson,[25] E. Thomson,[46] P. Tipton,[61] P. Ttito-Guzmán,[32] S. Tkaczyk,[18] D. Toback,[54] S. Tokar,[15] K. Tollefson,[36] T. Tomura,[56] D. Tonelli,[18] S. Torre,[20] D. Torretta,[18] P. Totaro[dd],[55] S. Tourneur,[45] M. Trovato,[47] S.-Y. Tsai,[1] Y. Tu,[46] N. Turini[aa],[47] F. Ukegawa,[56] S. Vallecorsa,[21] N. van Remortel[b],[24] A. Varganov,[35] E. Vataga[bb],[47] F. Vázquez[n],[19] G. Velev,[18] C. Vellidis,[3] M. Vidal,[32] R. Vidal,[18] I. Vila,[12] R. Vilar,[12] T. Vine,[31] M. Vogel,[38] I. Volobouev[t],[29] G. Volpi[z],[47] P. Wagner,[46] R.G. Wagner,[2] R.L. Wagner,[18] W. Wagner[w],[27] J. Wagner-Kuhr,[27] T. Wakisaka,[42] R. Wallny,[9] S.M. Wang,[1] A. Warburton,[34] D. Waters,[31] M. Weinberger,[54] J. Weinelt,[27] W.C. Wester III,[18] B. Whitehouse,[57] D. Whiteson[f],[46] A.B. Wicklund,[2] E. Wicklund,[18] S. Wilbur,[14] G. Williams,[34] H.H. Williams,[46] P. Wilson,[18] B.L. Winer,[40] P. Wittich[h],[18] S. Wolbers,[18] C. Wolfe,[14] T. Wright,[35] X. Wu,[21] F. Würthwein,[10] S. Xie,[33] A. Yagil,[10] K. Yamamoto,[42] J. Yamaoka,[17] U.K. Yang[p],[14] Y.C. Yang,[28] W.M. Yao,[29] G.P. Yeh,[18] J. Yoh,[18] K. Yorita,[58] T. Yoshida[m],[42] G.B. Yu,[50] I. Yu,[28] S.S. Yu,[18] J.C. Yun,[18] L. Zanello[cc],[52] A. Zanetti,[55] X. Zhang,[25] Y. Zheng[d],[9] and S. Zucchelli[x],[6]

(CDF Collaboration[†])

[†] With visitors from [a]University of Massachusetts Amherst, Amherst, Massachusetts 01003, [b]Universiteit Antwerpen, B-2610 Antwerp, Belgium, [c]University of Bristol, Bristol BS8 1TL, United Kingdom, [d]Chinese Academy of Sciences, Beijing 100864, China, [e]Istituto Nazionale di Fisica Nucleare, Sezione di Cagliari, 09042 Monserrato (Cagliari), Italy, [f]University of California Irvine, Irvine, CA 92697, [g]University of California Santa Cruz, Santa Cruz, CA 95064, [h]Cornell University, Ithaca, NY 14853, [i]University of Cyprus, Nicosia CY-1678, Cyprus, [j]University College Dublin, Dublin 4, Ireland, [k]University of Edinburgh, Edinburgh EH9 3JZ, United Kingdom, [l]University of Fukui, Fukui City, Fukui Prefecture, Japan 910-0017 [m]Kinki University, Higashi-Osaka City, Japan 577-8502 [n]Universidad Iberoamericana, Mexico D.F., Mexico, [o]Queen Mary, University of London, London, E1 4NS, England, [p]University of Manchester, Manchester M13 9PL, England, [q]Nagasaki Institute of Applied Science, Nagasaki, Japan, [r]University of Notre Dame, Notre Dame, IN 46556, [s]University de Oviedo, E-33007 Oviedo, Spain, [t]Texas Tech University, Lubbock, TX 79609, [u]IFIC(CSIC-Universitat de Valencia), 46071 Valencia, Spain, [v]University of Virginia, Charlottesville, VA 22904, [w]Bergische Universität Wuppertal, 42097 Wuppertal, Germany, [ee]On leave from J. Stefan Institute, Ljubljana, Slovenia,

[1]*Institute of Physics, Academia Sinica,*
Taipei, Taiwan 11529, Republic of China
[2]*Argonne National Laboratory, Argonne, Illinois 60439*
[3]*University of Athens, 157 71 Athens, Greece*
[4]*Institut de Fisica d'Altes Energies,*
Universitat Autonoma de Barcelona,
E-08193, Bellaterra (Barcelona), Spain
[5]*Baylor University, Waco, Texas 76798*
[6]*Istituto Nazionale di Fisica Nucleare Bologna,*
[x]*University of Bologna, I-40127 Bologna, Italy*
[7]*Brandeis University, Waltham, Massachusetts 02254*
[8]*University of California, Davis, Davis, California 95616*
[9]*University of California, Los Angeles, Los Angeles, California 90024*
[10]*University of California, San Diego, La Jolla, California 92093*
[11]*University of California, Santa Barbara, Santa Barbara, California 93106*
[12]*Instituto de Fisica de Cantabria, CSIC-University of Cantabria, 39005 Santander, Spain*
[13]*Carnegie Mellon University, Pittsburgh, PA 15213*
[14]*Enrico Fermi Institute, University of Chicago, Chicago, Illinois 60637*
[15]*Comenius University, 842 48 Bratislava,*
Slovakia; Institute of Experimental Physics, 040 01 Kosice, Slovakia
[16]*Joint Institute for Nuclear Research, RU-141980 Dubna, Russia*
[17]*Duke University, Durham, North Carolina 27708*
[18]*Fermi National Accelerator Laboratory, Batavia, Illinois 60510*
[19]*University of Florida, Gainesville, Florida 32611*
[20]*Laboratori Nazionali di Frascati, Istituto Nazionale*
di Fisica Nucleare, I-00044 Frascati, Italy
[21]*University of Geneva, CH-1211 Geneva 4, Switzerland*
[22]*Glasgow University, Glasgow G12 8QQ, United Kingdom*
[23]*Harvard University, Cambridge, Massachusetts 02138*
[24]*Division of High Energy Physics, Department of Physics,*
University of Helsinki and Helsinki Institute of Physics, FIN-00014, Helsinki, Finland
[25]*University of Illinois, Urbana, Illinois 61801*

[26]*The Johns Hopkins University, Baltimore, Maryland 21218*

[27]*Institut für Experimentelle Kernphysik,*
Universität Karlsruhe, 76128 Karlsruhe, Germany

[28]*Center for High Energy Physics: Kyungpook National University,*
Daegu 702-701, Korea; Seoul National University, Seoul 151-742,
Korea; Sungkyunkwan University, Suwon 440-746,
Korea; Korea Institute of Science and Technology Information, Daejeon,
305-806, Korea; Chonnam National University, Gwangju, 500-757, Korea

[29]*Ernest Orlando Lawrence Berkeley National Laboratory, Berkeley, California 94720*

[30]*University of Liverpool, Liverpool L69 7ZE, United Kingdom*

[31]*University College London, London WC1E 6BT, United Kingdom*

[32]*Centro de Investigaciones Energeticas*
Medioambientales y Tecnologicas, E-28040 Madrid, Spain

[33]*Massachusetts Institute of Technology, Cambridge, Massachusetts 02139*

[34]*Institute of Particle Physics: McGill University, Montréal,*
Québec, Canada H3A 2T8; Simon Fraser University, Burnaby,
British Columbia, Canada V5A 1S6; University of Toronto,
Toronto, Ontario, Canada M5S 1A7; and TRIUMF,
Vancouver, British Columbia, Canada V6T 2A3

[35]*University of Michigan, Ann Arbor, Michigan 48109*

[36]*Michigan State University, East Lansing, Michigan 48824*

[37]*Institution for Theoretical and Experimental Physics, ITEP, Moscow 117259, Russia*

[38]*University of New Mexico, Albuquerque, New Mexico 87131*

[39]*Northwestern University, Evanston, Illinois 60208*

[40]*The Ohio State University, Columbus, Ohio 43210*

[41]*Okayama University, Okayama 700-8530, Japan*

[42]*Osaka City University, Osaka 588, Japan*

[43]*University of Oxford, Oxford OX1 3RH, United Kingdom*

[44]*Istituto Nazionale di Fisica Nucleare, Sezione di Padova-Trento,*
[y]*University of Padova, I-35131 Padova, Italy*

[45]*LPNHE, Universite Pierre et Marie*
Curie/IN2P3-CNRS, UMR7585, Paris, F-75252 France

[46] University of Pennsylvania, Philadelphia, Pennsylvania 19104
[47] Istituto Nazionale di Fisica Nucleare Pisa, [z] University of Pisa,
[aa] University of Siena and [bb] Scuola Normale Superiore, I-56127 Pisa, Italy
[48] University of Pittsburgh, Pittsburgh, Pennsylvania 15260
[49] Purdue University, West Lafayette, Indiana 47907
[50] University of Rochester, Rochester, New York 14627
[51] The Rockefeller University, New York, New York 10021
[52] Istituto Nazionale di Fisica Nucleare, Sezione di Roma 1,
[cc] Sapienza Università di Roma, I-00185 Roma, Italy
[53] Rutgers University, Piscataway, New Jersey 08855
[54] Texas A&M University, College Station, Texas 77843
[55] Istituto Nazionale di Fisica Nucleare Trieste/Udine,
I-34100 Trieste, [dd] University of Trieste/Udine, I-33100 Udine, Italy
[56] University of Tsukuba, Tsukuba, Ibaraki 305, Japan
[57] Tufts University, Medford, Massachusetts 02155
[58] Waseda University, Tokyo 169, Japan
[59] Wayne State University, Detroit, Michigan 48201
[60] University of Wisconsin, Madison, Wisconsin 53706
[61] Yale University, New Haven, Connecticut 06520

(Dated: March 13, 2009)

Abstract

We present a measurement of the $t\bar{t}$ differential cross section with respect to the $t\bar{t}$ invariant mass, $d\sigma/dM_{t\bar{t}}$, in $p\bar{p}$ collisions at $\sqrt{s} = 1.96$ TeV using an integrated luminosity of 2.7 fb^{-1} collected by the CDF II experiment. The $t\bar{t}$ invariant mass spectrum is sensitive to a variety of exotic particles decaying into $t\bar{t}$ pairs. The result is consistent with the standard model expectation, as modeled by `PYTHIA` with `CTEQ5L` parton distribution functions.

PACS numbers: 13.85Rm,14.65Ha,14.80-j

The top quark is the only known fermion with a mass near the electroweak symmetry breaking (EWSB) scale [1]. As such, it plays a special role in many beyond the standard model (BSM) theories of EWSB. In the standard model (SM) the Higgs boson is responsible for EWSB and the generation of the fermion masses, but it has not yet been observed. In models with top condensation, such as technicolor and topcolor, the role of the SM Higgs boson is filled by a composite particle that is a bound state of top quarks [2]. These models predict additional heavy gauge bosons that couple strongly to top quarks. The hierarchy problem, also unresolved in the SM, has recently been addressed by models with extra dimensions, such as the Randall-Sundrum (RS) [3] and ADD models [4]. In these models TeV-scale gravitons can decay, in some cases preferentially, to $t\bar{t}$ pairs [5]. In all of these cases the production of $t\bar{t}$ pairs at hadron colliders through BSM mechanisms distorts the $t\bar{t}$ invariant mass spectrum relative to the SM expectation, as recently reviewed in [6].

In this Letter we report on the first measurement of the $t\bar{t}$ differential cross section with respect to the $t\bar{t}$ invariant mass, $d\sigma/dM_{t\bar{t}}$. The analysis uses an integrated luminosity of 2.70 ± 0.16 fb^{-1} [7] collected with the CDF II detector between March 2002 and April 2008. Full details of the analysis presented here are given in [8]. Previous published studies have focused on searches for resonances in the $M_{t\bar{t}}$ spectrum [9], and placed a lower limit of 720 GeV/c^2 on the mass of a putative Z' boson decaying preferentially to $t\bar{t}$. In this Letter we take a different approach in which we test the $M_{t\bar{t}}$ spectrum, generically, for consistency with the SM. In this way we are potentially sensitive to broad enhancements of the spectrum and interference effects [6], as well as to narrow resonances.

The CDF II detector is described in detail elsewhere [10]. The components relevant to this analysis include the silicon vertex detector (SVX), the central outer tracker (COT), the central electromagnetic and hadronic calorimeters, the central muon detectors, and the luminosity counters.

Because it allows reconstruction of the final state with good resolution, and because of the good signal to background ratio, we use the "lepton+jets" decay mode of the $t\bar{t}$ pair in this study. It consists of four energetic jets, two of which originate from bottom quarks and two from the hadronic W-boson decay, a charged lepton with large transverse momentum ($P_{\rm T}$), and a large transverse momentum imbalance ($\not\!\!E_T$) from the undetected neutrino from the leptonic W-boson decay [11]. Extra jets may appear from initial- or final-state radiation (ISR or FSR). A $t\bar{t}$ event may also be observed with fewer than four jets if a jet is not

reconstructed or is merged with another jet in the event. Monte Carlo (MC) simulations of $t\bar{t}$ production are generated using the PYTHIA MC program [12] with the CTEQ5L [13] parton distribution functions (PDFs). The decays of heavy quarks (b and c) are modeled using EVTGEN [14]. The HERWIG MC program [15] is used for studies of the systematic effects of the hadronization model. The $t\bar{t}$ MC samples are generated with a top quark mass of 175 GeV/c^2. The results presented here are insensitive to changes of the generated top quark mass of a few GeV/c^2.

Events from $p\bar{p}$ collisions are selected with an inclusive lepton trigger that requires an electron (muon) candidate with $E_{\rm T} > 18$ GeV ($P_{\rm T} > 18$ GeV/c). From the triggered events the signal sample is selected offline by requiring an isolated electron (muon) with $E_{\rm T} > 20$ GeV ($P_{\rm T} > 20$ GeV/c). The isolation criterion requires $I < 0.1$, where I is defined as the calorimeter transverse energy in a cone of opening radius $\Delta R \equiv \sqrt{(\Delta\eta)^2 + (\Delta\phi)^2} = 0.4$ around the lepton direction (exclusive of the lepton energy), divided by the electron (muon) $E_{\rm T}$ ($P_{\rm T}$). We further require $\not\!\!E_T > 20$ GeV and at least 4 jets each with $E_{\rm T} > 20$ GeV and $|\eta| < 2.0$. Jets are identified using a fixed-cone algorithm with a cone size of $\Delta R = 0.4$ and are constrained to originate at the $p\bar{p}$ collision vertex. Their energies are corrected to account for detector response variations in η, calorimeter gain instability, nonlinearity of calorimeter energy response, multiple interactions in an event, and for energy loss in un-instrumented regions of the detector. For events with more than four jets with $E_{\rm T} > 20$ GeV, we use the four highest-$E_{\rm T}$ jets in the $M_{t\bar{t}}$ reconstruction. Missing transverse energy is corrected to account for the shifts in jet energies due to the jet energy corrections described above. Z-boson candidate events are rejected by removing events containing a second isolated high-$P_{\rm T}$ lepton. To suppress the background from direct production of a W boson and multiple jets (W+jets events) we require that at least one jet in the event have an identified displaced secondary vertex, consistent with the decay of a B hadron. We label such jets, and the events that contain them, as "b-tagged". The events selected prior to the b-tag requirement are called "pretag" events. We observe 2069 pretag, and 650 b-tagged, events.

The $t\bar{t}$ signature described above can be mimicked by several processes, including diboson (WW, WZ, ZZ), single-top, Z+jets, and W+jets production, as well as processes without vector bosons to which we refer, generically, as "QCD" backgrounds. The diboson and single-top quark yields are predicted using PYTHIA and MADEVENT [16] MC samples, respectively, each normalized to the theoretical cross sections [17, 18]. The residual Z+jets background

is modeled using ALPGEN [19], with the parton showering and underlying event model from PYTHIA. The QCD background typically has lower $\not\!\!E_T$ than events with real W bosons and is evaluated by fitting the $\not\!\!E_T$ distribution using templates for QCD and W+jets sources and extrapolating the QCD fraction into the high-$\not\!\!E_T$ signal region. ALPGEN is also used in the evaluation of the dominant background from W+jets production. The W+jets background is determined separately for events with and without heavy-flavor jets. For events with heavy-flavor jets we use the ALPGEN simulation to determine the fraction, in each jet multiplicity bin, of W+jets events that are $Wb\bar{b}$, $Wc\bar{c}$ or Wc. This fraction is then increased by a correction factor, determined by comparing measured and ALPGEN-predicted heavy-flavor (HF) fractions in W+1 jet data. The number of pretag W+heavy-flavor events is normalized to the total number of W+jets events in each jet multiplicity bin of the data using the modified ALPGEN fractions. The background contribution from these events is given by the pretag number of events times a MC-derived tagging efficiency. Events without heavy-flavor jets can enter the signal sample if one of the jets is mistakenly b-tagged. Such events are called "mistags", and they occur primarily due to tracking errors, with a smaller contribution from interactions in the material of the detector, and K_S and Λ decays. The background due to mistags in W+jets events is evaluated using a measurement of the rate of mistags derived from multijet data [20]. The mistag rate is then applied to the number of pretag W+jets events, with no heavy-flavor jets, in the data. This pretag number is calculated, in each jet multiplicity bin, from the total number of candidate events corrected for the contributions from non-W+jets and from W+heavy-flavor jets. The observed event yields and background predictions are given in Tab. I, where the line labeled 'Other' includes dibosons, Z+jets and single top.

The precision of the measurement of $M_{t\bar{t}}$ depends on the understanding of the jet energy scale (JES). To reduce the uncertainty on the JES, we adopt an approach first used in [22] and use the measured invariant mass of the hadronically-decaying W boson to constrain the JES. For events with two b-tagged jets, the two un-tagged jets are chosen as the jets from the W boson decay. For events with a single b-tagged jet, the pair with invariant mass closest to the expected mean value from W boson decays is chosen. There are 503 single-tagged and 147 double-tagged events in the sample. An unbinned maximum likelihood fit, using MC templates for the dijet invariant mass distribution, for both signal and background, returns the best-fit JES and its uncertainty. The fit value of the JES is subsequently used in the analysis. The uncertainty returned by this procedure is approximately a factor of two lower

Process	4 jets	≥ 5 jets
W+HF	58.0 ± 12.2	11.6 ± 2.9
Mistags	18.9 ± 4.8	3.5 ± 1.6
QCD	20.9 ± 17.5	6.4 ± 6.0
Other	13.9 ± 0.8	3.1 ± 0.2
$t\bar{t}$ (6.7pb)	358.6 ± 49.7	121.5 ± 16.8
Total Prediction	470 ± 57	146 ± 19
Observed	494	156

TABLE I: Summary of sample composition [21].

than the nominal uncertainty on the JES.

We reconstruct $M_{t\bar{t}}$, the $t\bar{t}$ invariant mass, using the four-vectors of the b-tagged jet and the three remaining leading jets in the event, the lepton and the transverse components of the neutrino momentum, given by $\not\!\!E_T$. We divide the $M_{t\bar{t}}$ distribution into nine bins between 0 and 1400 GeV/c^2, with bin widths ranging from 50 GeV/c^2 for bins for which a large number of events are expected to 600 GeV/c^2 for the highest bin. The resolution in $M_{t\bar{t}}$ is somewhat smaller than the bin width, ranging from 11% near the peak to 15% at high mass. We subtract from the bulk $M_{t\bar{t}}$ distribution the expected contribution from the backgrounds listed in Tab. I, which is modeled using the Monte Carlo samples described above. The resulting $M_{t\bar{t}}$ signal distribution suffers from resolution smearing and is corrected using a regularized unfolding technique, described below, which also accounts for the longitudinal component of the neutrino momentum.

In order to extract the true underlying $M_{t\bar{t}}$ distribution from the background-subtracted reconstructed distribution, we use the MC to create a response matrix $\hat{A}$, such that $\hat{A}x = d$ where x is the true, binned distribution and d is the measured, binned distribution. Due to statistical fluctuations in bins with small numbers of events, inverting the response matrix $\hat{A}$ to solve for x given d often yields spurious results. Instead we use singular-value decomposition (SVD) unfolding, as described in [23], where the solution is regularized by populating the response matrix with event multiplicities instead of probabilities. The application to this analysis is described in detail in [8].

From the unfolded $M_{t\bar{t}}$ distribution, we calculate the differential cross section according

to

$$\frac{d\sigma^i}{dM_{t\bar{t}}} = \frac{N_i}{\mathcal{A}_i \int \mathcal{L}dt \cdot \Delta^i_{M_{t\bar{t}}}}, \quad (1)$$

where N_i is the background-subtracted, unfolded, number of events observed in each bin; $\mathcal{A}_i$ is the acceptance in bin i; $\Delta^i_{M_{t\bar{t}}}$ is the width of bin i; and $\int \mathcal{L}$dt is the integrated luminosity. The acceptance is measured from a mixture of data and MC. We use PYTHIA with a GEANT-based [20] detector simulation to measure the geometric and kinematic acceptance. The lepton trigger and identification efficiencies are measured in data using $Z \to \ell\ell$ decays. We account for the difference in efficiency for identifying an isolated high-$P_{\rm T}$ lepton in data and MC with a scale factor. Similarly we use a scale factor to correct for the difference in efficiency in data and MC for tagging a b-jet. The efficiency in data is determined in a heavy-flavor-enriched data sample of low-$P_{\rm T}$ electrons, from the semi-leptonic decay of B hadrons.

Our systematic uncertainties arise from MC modeling of the acceptance, true and reconstructed $M_{t\bar{t}}$ distributions, and background distributions. In addition, the uncertainties of our efficiency of lepton identification, b-tagging efficiency, and integrated luminosity affect the measurement. The lepton identification uncertainty arises due to the extrapolation from $Z \to \ell\ell$ events, where the efficiency is measured in data, to the higher multiplicity $t\bar{t}$ environment. The uncertainty on the b-tagging efficiency is largely due to the limited number of events in the data sample that is used. These uncertainties, together with a small uncertainty due to the finite size of the MC simulation used to calculate the acceptance, comprise the acceptance uncertainty in Tab. II.

We consider several variations to the MC model of the signal and background. For the signal MC simulation we compare the results using HERWIG to the default PYTHIA generator. The uncertainty due to the limited knowledge of ISR is constrained by studies of radiation in Drell-Yan events in the data. We vary both ISR and FSR within these limits and add the deviations from the nominal value in quadrature. The uncertainty due to possible differences in the PDFs from the nominal CTEQ5L PDF is evaluated by varying the PDF using the 20 CTEQ5L eigenvectors, which represent 90% C.L. variations. The deviations from the nominal values are added in quadrature with deviations measured using the MRST PDF [24] with two alternate choices for the strong coupling constant. The uncertainty on the background prediction consists of two pieces: the uncertainty on the background

normalization, given in Tab. I, and a background shape systematic for the MC modeling of the shapes. The systematic uncertainty due to the JES includes a generic energy-correction systematic uncertainty as well as a contribution from the modeling of the b-jet energy scale. The effects of each systematic uncertainty on the measurement are evaluated using a pseudo-experiment approach. Pseudo-experiments are performed for each variation described above and the difference between the mean $d\sigma/dM_{t\bar{t}}$ in each bin with the shifted parameters and the default model is taken as the systematic uncertainty in that bin. The results are presented in Tab. II. The dominant systematic uncertainty is the uncertainty on the PDF set. This is expected as the tail of the $M_{t\bar{t}}$ spectrum is very sensitive to the PDFs. The 6% uncertainty on the luminosity measurement in each bin [7] is not included in the total in Tab. II. Two effects cause the uncertainty in the bins between 400 GeV/c^2 and 550 GeV/c^2 to be somewhat smaller than outside of that range. One is the turn-on threshold of the $M_{t\bar{t}}$ spectrum, which is insensitive to systematic variations because we fix the top quark mass at 175 GeV/c^2. The second is the PDF uncertainty, which is much greater at large $M_{t\bar{t}}$ than at small $M_{t\bar{t}}$.

$M_{t\bar{t}}$ [GeV/c^2]	0-350	350-400	400-450	450-500	500-550	550-600	600-700	700-800	800-1400
MC Gen.	0.7	2.4	5.3	5.7	4.6	3.3	1.4	1.0	1.0
ISR/FSR	1.5	1.3	0.8	0.2	1.1	2.1	2.0	2.2	3.3
JES	8.2	6.3	4.1	3.1	1.7	2.3	4.6	7.5	9.1
Backgrounds	10.3	7.4	2.4	1.7	3.0	4.0	4.5	5.1	5.4
Acceptance	4.5	4.4	4.3	4.4	4.6	4.6	4.4	4.0	3.8
PDF Set	7.7	6.1	3.0	1.0	4.8	9.3	14.0	17.4	18.8
Total	16.0	12.6	8.9	8.1	8.9	12.0	16.1	20.1	22.2

TABLE II: Summary of systematic uncertainties (in %) in each bin. The 6% uncertainty on the integrated luminosity is not included in the total.

The measured $d\sigma/dM_{t\bar{t}}$ is shown in Fig. 1 and tabulated in Tab. III.

We check consistency with the SM prediction using the Anderson-Darling (AD) statistic [25], which places an emphasis on potential discrepancies in the tail of the $M_{t\bar{t}}$ distribution. The distribution of the AD statistic for this analysis is rapidly falling, with small values corresponding to more likely results. Using MC simulations, we optimize the bin range of the Anderson-Darling statistic for maximum sensitivity to new physics and a minimum of false

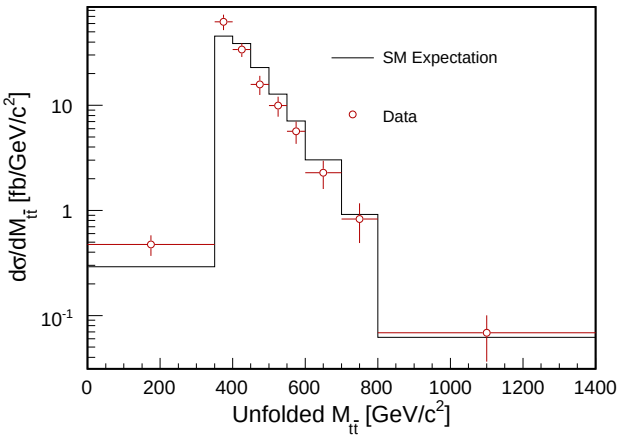

FIG. 1: $d\sigma/dM_{t\bar{t}}$ measured with 2.7 fb^{-1} of integrated luminosity.

$M_{t\bar{t}}$ [GeV/c^2]	$\mathcal{A}_i$	$d\sigma/dM_{t\bar{t}}$ [fb/GeV/c^2]
$\leq$ 350	0.016±0.001	0.47 ± 0.07 ± 0.08 ± 0.03
350-400	0.023±0.001	62.3 ± 7.0 ± 7.9± 3.7
400-450	0.026±0.001	33.8 ± 4.0 ± 3.0 ± 2.0
450-500	0.027±0.001	15.8 ± 3.0 ± 1.3 ± 0.9
500-550	0.029±0.001	9.9 ± 2.0 ± 0.9 ± 0.6
550-600	0.030±0.001	5.7 ± 1.2 ± 0.7 ± 0.3
600-700	0.030±0.001	2.3 ± 0.6 ± 0.4 ± 0.1
700-800	0.030±0.001	0.8 ± 0.3 ± 0.2 ± 0.1
800-1400	0.023±0.001	0.068 ± 0.032 ± 0.015 ± 0.004
Integrated Cross Section [pb] 6.9 ± 1.0 (stat.+JES)		

TABLE III: The acceptance and measured differential cross section in each bin. The uncertainties on the cross-section values are, respectively, statistical+JES, systematic and luminosity.

positives and find $M_{t\bar{t}} \geq 450$ GeV/c^2 to be the most sensitive region of $M_{t\bar{t}}$. We perform pseudo-experiments using the SM MC distributions of $M_{t\bar{t}}$ with the sample composition given in Tab. I. We calculate a p-value by taking the fraction of pseudo-experiments with a larger observed (*i.e.* less likely in the SM) Anderson-Darling statistic than that in data. The observed p-value is 0.28. We conclude that there is no evidence of non-SM physics in

the $M_{t\bar{t}}$ distribution.

We thank Rikkert Frederix, Fabio Maltoni, and Tim Stelzer for stimulating discussions, advice, and help with MadEvent generation. We thank the Fermilab staff and the technical staffs of the participating institutions for their vital contributions. This work was supported by the U.S. Department of Energy and National Science Foundation; the Italian Istituto Nazionale di Fisica Nucleare; the Ministry of Education, Culture, Sports, Science and Technology of Japan; the Natural Sciences and Engineering Research Council of Canada; the National Science Council of the Republic of China; the Swiss National Science Foundation; the A.P. Sloan Foundation; the Bundesministerium für Bildung und Forschung, Germany; the Korean Science and Engineering Foundation and the Korean Research Foundation; the Science and Technology Facilities Council and the Royal Society, UK; the Institut National de Physique Nucleaire et Physique des Particules/CNRS; the Russian Foundation for Basic Research; the Ministerio de Ciencia e Innovación, and Programa Consolider-Ingenio 2010, Spain; the Slovak R&D Agency; and the Academy of Finland.

---

[1] C. Amsler *et al.*, Phys. Lett. B **667**, 1 (2008).

[2] G. Cvetic, Reviews of Modern Physics **71**, 513(1999).

[3] L. Randall and R. Sundrum, Phys. Rev. Lett., **83**, 3370 (1999).

[4] N. Arkani-Hamed, S. Dimopoulos and G. R. Dvali, Phys. Lett. B **429**, 263 (1998).

[5] L. Fitzpatrick, J. Kaplan, L. Randall, L. Wang, JHEP **0709**, 013 (2007).

[6] R. Frederix and F. Maltoni, JHEP **0901**, 047 (2009).

[7] S. Klimenko, J. Konigsberg, and T.M. Liss, Fermilab-FN-0741.

[8] Alice Patricia Bridgeman, Measurement of the $t\bar{t}$ Differential Cross Section, $d\sigma/dM_{t\bar{t}}$, in $p\bar{p}$ Collisions at $\sqrt{s} = 1.96$ TeV, Ph.D Thesis, University of Illinois at Urbana-Champaign, 2008. FERMILAB-THESIS-2008-50

[9] T. Aaltonen *et al.*, (CDF Collaboration), Phys. Rev. D **77**, 051102(R) (2008); V.M. Abazov *et al.*, (DØ Collaboration), Phys. Lett. B **668**, 98 (2008).

[10] The CDF II Detector Technical Design Report, Fermilab-Pub-96/390-E; D. Amidei *et al.*, Nucl. Instum. Methods Phys. Res. A **350**, 73 (1994); F. Abe *et al.*, Phys. Rev. D **52**, 4784 (1995); P. Azzi *et al.*, Nucl. Instrum. Methods Phys. Res. A **360**, 137 (1995); D. Acosta *et al.*,

Phys. Rev. D **71**, 032001 (2005).

[11] We use a coordinate system where the z-axis is in the direction of the proton beam, and ϕ and θ are the azimuthal and polar angles respectively. The pseudorapidity, η, is defined as $\eta = -\ln(\tan\frac{\theta}{2})$. The transverse momentum of a charged particle is $P_{\rm T} = P\sin\theta$, where P represents the measured momentum of the charged-particle track. The analogous quantity using calorimeter energies, defined as $E_T = E\sin\theta$, is called transverse energy. The missing transverse energy is defined as $\not\!\!E_T = -\mid \sum_i E_T^i \hat{n}_i \mid$ where E_T^i is the magnitude of the transverse energy contained in each calorimeter tower i in the pseudorapidity region $\mid \eta \mid < 3.6$, and $\hat{n}_i$ is the direction unit vector of the tower in the plane transverse to the beam direction.

[12] T. Sjöstrand, S. Mrenna, and P. Skands, JHEP **0605**, 026 (2006). We use PYTHIA version 6.216.

[13] H. L. Lai *et al.* (CTEQ Collaboration), Eur. Phys. J. C **12**, 375 (2000).

[14] D. J. Lange, Nucl. Instrum. Meth. A **462**, 152 (2001).

[15] G. Corcella *et al.*, JHEP **0101**, 010 (2001).

[16] J. Alwall *et al.*, JHEP **0709**, 028 (2007).

[17] J. M. Campbell and R. K. Ellis, Phys. Rev. D **60**, 113006 (1999).

[18] Z. Sullivan, Phys. Rev. D **70**, 114012 (2004).

[19] M.L. Mangano *et al.*, JHEP **0307**, 001 (2003).

[20] D. Acosta *et al.*, (CDF Collaboration), Phys. Rev. D **71**, 052003 (2005).

[21] CDF Conference Note 9462, `http://www-cdf.fnal.gov/physics/new/top/2008/xsection/ttbar_secvtx_3invfb/`

[22] A. Abulencia *et al.*, (CDF Collaboration), Phys. Rev. Lett. **96**, 022004 (2006); A. Abulencia *et al.*, (CDF Collaboration), Phys. Rev. D **73**, 032003 (2006).

[23] A. Hocker and V. Kartvelishivili, hep-ph/9509307 (1995).

[24] A. D. Martin *et al.*, Eur. Phys. J. C **14**, 133 (2000).

[25] T. W. Anderson and D. A. Darling, The Annals of Math. Stat. **23**, 193 (1952).